ISSN 0915-633X

NATIONAL INSTITUTE FOR FUSION SCIENCE

Wakefield of a Charged Particulate Influenced by Emission Process of Secondary Electrons

K. Nishimura

(Received - Dec. 15, 1999)

NIFS-625 Mar. 2000

RESEARCH REPORT
NIFS Series

NAGOYA, JAPAN

Wakefield of a charged particulate influenced by emission process of secondary electrons

Kazumi Nishimura

Theory and Computer Simulation Center, National Institute for Fusion Science Toki 509-5292, Japan

abstract

Wakefield of a charged particulate in a streaming plasma is investigated by a three-dimensional particle simulation A difference is found in wakefields between a negatively charged particulate and a positively charged one, depending on the velocity of the particulate relative to that of the streaming plasma.

KEYWORDS dusty plasma, plasma crystal, wakefield, particle simulation

The realization of a "plasma crystal" in experimental plasma has made the ordered structure of dusty plasmas visible to naked eyes [1–4] Since then, dusty plasma has been one of the attractive subjects of study in plasma physics. Particulates immersed in a plasma acquire a charge from the surrounding plasma and interact with other particulates through an isotropic screened Coulomb potential if there is no external force In actual experiments on plasma crystals, an anisotropic layered structure of particulates can be observed in the vicinity of the sheath region where ion flow exists It has been pointed out that plasma flow disturbs the Coulomb potential of a charged particulate. In particular, when the velocity of plasma flow becomes greater than the ion-acoustic velocity c_s $(= \sqrt{k_B T_e/m_i}$, where $k_B T_e$ is the electron thermal energy and m_i is the ion mass), a potential structure called a "wakefield" can be generated on the downstream side of a particulate [5–8]. While it is said that the layered structure that appears in a plasma crystal results from the wakefield, there is no direct evidence to support this assertion.

The mechanism by which the wakefield is generated can be explained by a theory similar to that for the Cherenkov emission [9]. To put it briefly, a charged particulate in a plasma can emit an ion-acoustic wave under conditions where the velocity of the particulate relative to that of the plasma becomes greater than the ion-acoustic velocity. Analysis shows that an oscillatory structure of the electric potential appears on the downstream side of a test particle and the characteristic length of the wakefield is determined only by the relative velocity [6,7].

An electrostatic fluid simulation [10] and a Monte Carlo simulation [11] were carried out, in which the particulate charge was fixed to be negative, and the formation of the wakefield was confirmed. The process of charging of a particulate in a plasma has been studied through particle simulations [12,13]. Lapenta [13] verified the generation of the wakefield for negatively charged particulates using his elaborate simulation code. In most experiments on plasma crystals, particulates in plasmas charge up negatively because the mobility of electrons is larger than that of ions.

There are some effects which can make the particulate charge positive. Electrons hitting the particulate may cause secondary electrons to be emitted from inside the particulate (secondary electron emission) [14,15]. Furthermore, electrons inside the particulate can be emitted from the surface when the particulate is heated (thermionic emission) [16] or when the particulate is exposed to light (photoemission) [17]

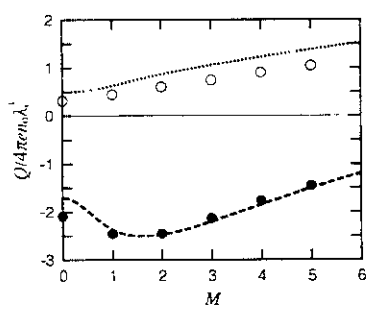

Fig. 1 Dependence of the equilibrium charge of a particulate $Q/4\pi\epsilon n_0\lambda_s^3$ on the Mach number M Both the simulation results (circles) and the analytical results (lines) are shown for two different values of δ_M : $\delta_M = 0$ (closed circles and broken line) and $\delta_M = 10$ (open circles and dotted line)

When these effects are essential to the charging process, the particulate charge can become positive. Little attention has been given to the wakefield generated by a positively charged particulate until now. Our concern is to investigate the wakefield created by a charged particulate immersed in a streaming plasma and discuss some of the differences between the wakefields generated by a positively charged particulate and a negatively charged one. We perform a three-dimensional particle simulation dealing with both attachment of plasma particles and emission of secondary electrons from the surface of a particulate.

Our numerical scheme is a standard particle simu-

lation based on the particle-in-cell (PIC) method [18]. We treat plasma particles (ions and electrons) as superparticles, the loaded number of which is 3×10^6 for each species. A rectangular simulation domain ($L_x \times L_y \times L_z$) is divided into $65 \times 65 \times 129$ grids. The simulation region is $L_x = L_y = 32\lambda_e$ and $L_z = 64\lambda_e$, where λ_e is the electron Debye length, then the grid separations are uniform, $\Delta x = \Delta y = \Delta z = 0.5\lambda_e$. Periodic conditions are imposed at all of the boundaries. We assume one spherical particulate with finite radius a to be at rest in a plasma, the position of which $R_d = (16\lambda_e, 16\lambda_e, 48\lambda_e)$ is fixed throughout this calculation. The equations to be solved are the equations of motion of both the ions and the electrons, and Poisson's equation. The charge density of the plasma ρ_p is defined at space grids by summing up all of the superparticles. The particulate charge is also assigned to space grids to obtain the charge density ρ_d, where a quadratic spline is used for an interpolating function [18].

The temporal evolution of the particulate charge is controlled by the following model. When the position of a plasma particle r satisfies the condition, $|r - R_d| \leq a$, this particle is regarded as absorbed into the particulate and is excluded from the calculation thereafter. The charge of the absorbed particle is added to the particulate charge. On the other hand, when one electron is absorbed into the particulate, new electrons with thermal energy kT_s are released from the particulate surface and added to the calculation thereafter. The charge of the released electrons is subtracted from the particulate charge. The electron yield $\delta(E)$, i.e., the ratio of secondary electrons to primary ones, is determined by the widely used formula,

$$\delta(E) = 7.4\delta_M \frac{E}{E_M} \exp(-2\sqrt{E/E_M}), \qquad (1)$$

where E is the primary electron energy, δ_M and E_M are parameters depending on the material of a particulate [14].

We assume the initial ion distribution is shifted Maxwellian with spatially constant temperature T_i, and the drift velocity is equal to the flow velocity V which is in the negative z direction. On the other hand, the electron distribution is assumed to be Maxwellian with spatially constant temperature T_e. The flow velocity considered in this letter satisfies the condition, $v_{Ti} < V < v_{Te}$, where v_{Ti} and v_{Te} are the ion and electron thermal velocity, respectively. From now on, we express the flow velocity using the Mach number, $M = V/c_s$. The typical simulation parameters are as follows: the mass ratio is $m_i/m_e = 50$, the charge ratio is $q_i/e = 1$, the temperature ratio is $T_i/T_e = 0.1$, the radius of the particulate is $a/\lambda_e = 1$, the ratio of thermal velocities is $v_{Ti}/v_{Te} = 0.045$, and the ion-acoustic velocity is $c_s/v_{Te} = 0.141$. The time step for integrating the equations of motion is $\omega_{pe}\Delta t = 0.05$ ($\omega_{pe} = \sqrt{4\pi e^2 n_0/m_e}$, where n_0 is the averaged number density of electrons). With these parameters, we use the following parameters for the emission of secondary electrons: $E_M/kT_e = 100$, $T_s/T_e = 0.5$. The number of emitted electrons can be determined freely by changing the parameter δ_M.

Figure 1 shows the relation between the equilibrium charge of a particulate and the Mach number. The closed circles ($\delta_M = 0$) and the open circles ($\delta_M = 10$) correspond to the results of our particle simulation. The particulate charge is zero initially, then it reaches an equilibrium value after $t \sim 10\omega_{pe}^{-1}$. The level of fluctuation is about a few percent of the equilibrium

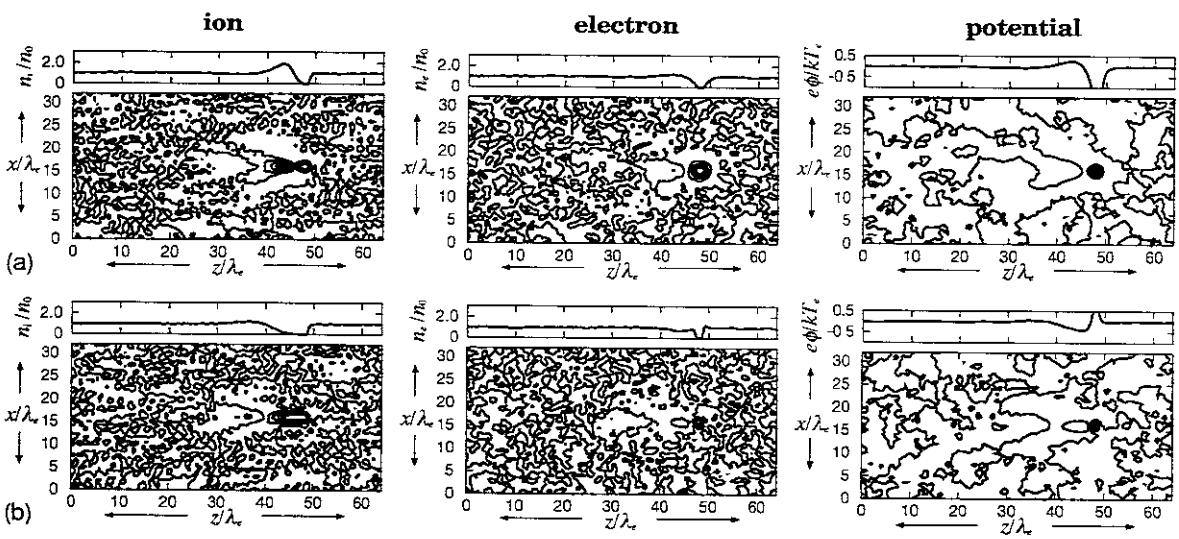

Fig. 2. Contour plots of ion density, electron density, and electric potential at $M = 3$ for two different values of δ_M (a) $\delta_M = 0$, negatively charged particulate and (b) $\delta_M = 10$, positively charged particulate. The upper and lower parts on each figure show the normalized quantity in the z direction at $(x, y) = (L_x/2, L_y/2)$ and the contour on the $y = L_y/2$ plane, respectively

charge. We carried out our simulation until $t = 100\omega_{pe}^{-1} \sim 150\omega_{pe}^{-1}$, when ions at $z \simeq L_z$ initially with drift velocity $v_z = -V$ come up to $z \simeq 0$. A particulate charges up by absorbing surrounding ions and electrons, then the surface charge without electron yield ($\delta_M = 0$) becomes negative because of the larger mobility of electrons than that of ions. On the other hand, when the emission of electrons is efficient ($\delta_M = 10$), the particulate charge remains a positive value. The number of particles absorbed on the particulate tends to increase as the Mach number increases. The lines in Fig. 1 show the analytical results obtained from the current balance equation, $I_i + I_e + I_s = 0$, where I_i, I_e, and I_s are the total current of ions, electrons, and secondary electrons, respectively, towards the particulate surface for $\delta_M = 0$ (broken line) and $\delta_M = 10$ (dotted line) [14,19,20]. It is found that our simulation results show good agreement with the theoretical prediction.

Figure 2 shows the density distribution of the ions and electrons, and the electric potential structure for (a) a negatively charged particulate ($\delta_M = 0$) and (b) a positively charged one ($\delta_M = 10$) at $M = 3$. The upper and lower parts on each figure show the normalized quantity in the z direction at $(x, y) = (L_x/2, L_y/2)$ and the contour on the $y = L_y/2$ plane, respectively. These quantities are averaged over a long time interval to remove the numerical noise.

To begin with, we shall discuss the negatively charged particulate in Fig. 2(a). The ion focus region clearly appears right on the downstream side of the particulate. It is also found that the shape of the disturbance is conical, the top angle of which agrees with the Mach angle α, i.e., $\sin\alpha = 1/M$. The electron distribution slightly deforms from the Boltzmann distribution and the focus region appears on the downstream side. We can see that the potential structure deforms from the isotropic potential and the conical structure shown in the ion density distribution appears also in the potential distribution. It is important to note that a peak of the potential exists on the downstream side, where the electric field E_z becomes zero.

Next, we shall discuss the property of these quantities for a positively charged particulate in Fig. 2(b). The region of rare ion density on the downstream side becomes large compared with that in Fig. 2(a) because the positively charged particulate repels ions. It is also found that the electron density does not decrease around a particulate as much as the ion density does. In our model, the number of secondary electrons is almost the same as that of primary ones when $\delta_M = 10$, and secondary electrons are emitted from the position on the particulate surface where a primary electron is absorbed. Therefore, the electron density does not decrease even if many electrons are absorbed on the particulate. We can see the negative region and a bottom of the electric potential on the downstream side.

Let us focus on the electric field created by the wake-field. As shown in Fig. 2, there appears a peak or a bottom of the electric potential on the downstream side, where the electric field E_z becomes zero. The distance

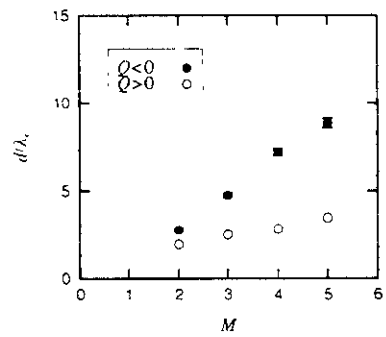

Fig. 3 Dependence of the distance d/λ_e from a particulate surface to the closest zero point of the electric field on the Mach number M for the same case as Fig. 1

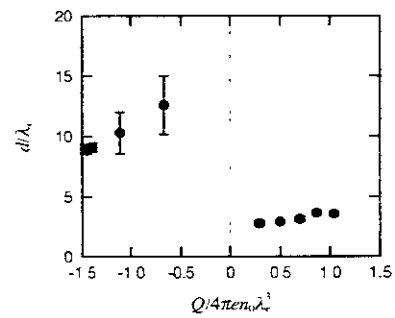

Fig. 4. Dependence of the distance d/λ_e on the particulate charge $Q/4\pi\varepsilon n_0\lambda_e^3$ at $M = 5$ for various values of δ_M

d/λ_e from the particulate surface to the nearest position of $E_z = 0$ varies for various Mach numbers. This relation is shown in Figure 3, where the closed and open circles correspond to those in Fig. 1. The important point is that the difference between a negatively charged particulate and a positively charged one becomes remarkable as the Mach number increases. It is clear that the distance for a negatively charged particulate tends to be larger than that for a positively charged particulate.

Figure 4 shows the dependence of the distance d/λ_e on the particulate charge at $M = 5$, where we changed δ_M from 0 to 10 to obtain various values of the particulate charge. When the charge is positive, the distances are almost same, regardless of various values of the charge. On the other hand, when the charge is negative, the distances are changed slightly, depending on the absolute values of the charge. It is obvious that there exists a clear difference about the distances between negatively charged particulates and positively charged ones, irrelevant to the absolute values of the charge. Although we must draw attention to the border of sign of the charge, we cannot observe a clear wake-field emitted by a particulate whose charge is almost comparable with the fluctuation. Thus, we have no re-

liable information on the distance d/λ_e in the vicinity of $Q \sim 0$. It should be concluded, from Figs. 3 and 4, that the difference of wakefields emitted by a negatively charged particulate and a positively charged one can be characterized by the velocity of the particulate relative to that of the plasma, irrelevant to the absolute value of the particulate charge.

There is an assertion that the anisotropy of a plasma crystal is caused by the wakefield, namely the distance d/λ_e corresponds to the length between the layers observed in a plasma crystal [6,7]. As our simulation results show, the length between layers will depend on both the Mach number and the sign of the dust charge if this assertion is true. Thus, an experiment in which the Mach number or the sign of the particulate charge is changed could answer the question as to whether the layered structure of a plasma crystal can be explained as being attributable to the wakefield.

In summary, we have investigated the wakefield created by a particulate immersed in a streaming plasma by means of a three-dimensional particle simulation. Considering the effect of secondary electron emission in the charging process, we have explored the outcome in the case of both positively and negatively charged particulates. It has been found that the difference of the wakefield between two cases can be characterized in terms of the velocity of the particulate relative to that of the plasma, irrelevant to the absolute value of the particulate charge.

The author would like to express his gratitude to Prof. T. Sato for providing him the opportunity to study at the Theory and Computer Simulation Center, National Institute for Fusion Science. He also acknowledges helpful discussions with Drs. Y. Todo and T.-H. Watanabe, and valuable advice offered by Drs. S. Ishiguro and H. Takamaru.

[1] J. H. Chu and Lin I, Phys. Rev. Lett. **72**, 4009 (1994).
[2] H. Thomas, G. E. Morfill, and V. Demmel, Phys. Rev. Lett. **73**, 652 (1994).
[3] Y. Hayashi and K. Tachibana, Jpn. J. Appl. Phys. **33**, L804 (1994).
[4] A. Melzer, T. Trottenberg, and A. Piel, Phys. Lett. A **191**, 301 (1994)
[5] O. Havnes, et al., J. Geophys. Res. 100 (1995) 1731.
[6] P. K. Shukla and N. N. Rao, Phys. Plasmas 3 (1996) 1770.
[7] O. Ishihara and S. V. Vladimirov, Phys. Plasmas **4**, 69 (1997).
[8] A. Melzer, V. A. Schweigert, and A. Piel, Phys. Rev. Lett. **83**, 3194 (1999).
[9] N. A. Krall and A. W. Trivelpiece, *Principles of Plasma Physics* (McGraw-Hill, New York, 1973) p.562.
[10] F. Melandsø and J. Goree, Phys. Rev. E **52**, 5312 (1995).
[11] A. Melzer, V. A. Schweigert, I. V. Schweigert, A. Homann, S. Peters, and A. Piel, Phys. Rev. E **54**, R46 (1996).
[12] B. Young, T. E. Cravens, T. P. Armstrong, and R. J. Friauf, J. Geophys. Res. **99**, 2255 (1994)
[13] G. Lapenta, Phys. Plasmas **6**, 1442 (1999).
[14] N. Meyer-Vernet, Astron. Astrophys. **105**, 98 (1982).
[15] K. Watanabe, K. Nishimura, and T. Sato, in *Advances in Dusty Plasmas*, edited by P K Shukla, D. A. Mendis, and T. Desai (World Scientific, Singapore, 1997), p.394.
[16] V. E. Fortov, A. P. Nefedov, O. F. Petrov, A. A. Samarian, and A. V. Chernyschev, Phys. Rev. E **54**, R2236 (1996).
[17] M. Rosenberg, IEEE Trans. Plasma Sci. **24**, 1422 (1996)
[18] C. K. Birdsall and A. B. Langdon, *Plasma Physics via Computer Simulation* (IOP Publishing, Bristol and Philadelphia, 1991).
[19] J. R. Hill and D. A. Mendis, Moon Planets **21**, 3 (1979)
[20] E. C. Whipple, Rep Prog Phys. **44**, 1197 (1981).

Recent Issues of NIFS Series

NIFS-562 S. Yoshikawa,
Next Generation Toroidal Devices, Oct 1998

NIFS-563 Y Todo and T Sato,
Kinetic-Magnetohydrodynamic Simulation Study of Fast Ions and Toroidal Alfvén Eigenmodes; Oct 1998
(IAEA-CN-69/THP2/22)

NIFS-564 T Watari, T Shimozuma, Y Takeiri, R Kumazawa, T Mutoh, M Sato, O Kaneko, K Ohkubo, S. Kubo, H Idei, Y Oka, M Osakabe, T. Seki, K Tsumori, Y Yoshimura, R Akiyama, T. Kawamoto, S Kobayashi, F Shimpo, Y Takita, E Asano, S. Itoh, G Nomura, T. Ido, M. Hamabe, M Fujiwara, A Iiyoshi, S Morimoto, T Bigelow and Y P Zhao,
Steady State Heating Technology Development for LHD, Oct 1998
(IAEA-CN-69/FTP/21)

NIFS-565 A Sagara, K.Y. Watanabe, K Yamazaki, O Motojima, M. Fujiwara, O Mitarai, S Imagawa, H Yamanishi, H Chikaraishi, A Kohyama, H. Matsui, T Muroga, T. Noda, N Ohyabu, T Satow, A.A Shishkin, S. Tanaka, T Terai and T Uda,
LHD-Type Compact Helical Reactors, Oct 1998
(IAEA-CN-69/FTP/03(R)

NIFS-566 N. Nakajima, J Chen, K Ichiguchi and M. Okamoto,
Global Mode Analysis of Ideal MHD Modes in L=2 Heliotron/Torsatron Systems, Oct 1998
(IAEA-CN-69/THP1/08)

NIFS-567 K Ida, M. Osakabe, K Tanaka, T Minami, S. Nishimura, S. Okamura, A Fujisawa, Y. Yoshimura, S. Kubo, R Akiyama, D.S Darrow, H Idei, H Iguchi, M. Isobe, S. Kado, T Kondo, S. Lee, K Matsuoka, S. Morita, I. Nomura, S. Ohdachi, M Sasao, A Shimizu, K Tumori, S. Takayama, M Takechi, S. Takagi, C Takahashi, K Toi and T Watari,
Transition from L Mode to High Ion Temperature Mode in CHS Heliotron/Torsatron Plasmas; Oct 1998
(IAEA-CN-69/EX2/2)

NIFS-568 S. Okamura, K Matsuoka, R Akiyama, D.S. Darrow, A Ejiri, A Fujisawa, M. Fujiwara, M. Goto, K Ida H Idei, H. Iguchi, N Inoue, M. Isobe, K Itoh, S. Kado, K Khlopenkov, T. Kondo, S. Kubo, A Lazaros, S Lee, G. Matsunaga, T. Minami, S. Morita, S Murakami, N. Nakajima, N Nikai, S. Nishimura, I. Nomura, S. Ohdachi, K Ohkuni, M. Osakabe, R. Pavlichenko, B Peterson, R Sakamoto, H. Sanuki, M. Sasao, A Shimizu, Y Shirai, S. Sudo, S. Takagi, C. Takahashi, S Takayama, M. Takechi, K Tanaka, K Toi, K Yamazaki, Y. Yoshimura and T. Watari,
Confinement Physics Study in a Small Low-Aspect-Ratio Helical Device CHS, Oct. 1998
(IAEA-CN-69/OV4/5)

NIFS-569 M.M. Skoric, T. Sato, A Maluckov, M S. Jovanovic,
Micro- and Macro-scale Self-organization in a Dissipative Plasma; Oct 1998

NIFS-570 T. Hayashi, N. Mizuguchi, T-H. Watanabe, T. Sato and the Complexity Simulation Group,
Nonlinear Simulations of Internal Reconnection Event in Spherical Tokamak, Oct 1998
(IAEA-CN-69/TH3/3)

NIFS-571 A Iiyoshi, A. Komori, A Ejiri, M Emoto, H. Funaba, M Goto, K Ida, H Idei, S. Inagaki, S. Kado, O Kaneko, K Kawahata, S Kubo, R Kumazawa, S. Masuzaki, T. Minami, J. Miyazawa, T Morisaki, S. Morita, S. Murakami, S Muto, T Muto, Y. Nagayama, Y Nakamura, H. Nakanishi, K Narihara, K. Nishimura, N. Noda, T Kobuchi, S. Ohdachi, N. Ohyabu, Y. Oka, M. Osakabe, T. Ozaki, B.J. Peterson, A Sagara, S. Sakakibara, R Sakamoto, H. Sasao, M Sasao, K Sato, M. Sato, T Seki, T Shimozuma, M. Shoji, H. Suzuki, Y. Takeiri, K Tanaka, K Toi, T. Tokuzawa, K Tsumori, I. Yamada, H. Yamada, S Yamaguchi, M. Yokoyama, K.Y.Watanabe, T Watari, R Akiyama, H. Chikaraishi, K Haba, S. Hamaguchi, S Iima, S. Imagawa, N Inoue, K Iwamoto, S. Kitagawa, Y. Kubota, J. Kodaira, R. Maekawa, T Mito T Nagasaka, A Nishimura, Y Takita, C Takahashi, K Takahata, K Yamauchi, H Tamura, T. Tsuzuki, S Yamada, N Yanagi, H Yonezu, Y Hamada, K Matsuoka, K Murai, K Ohkubo, I Ohtake, M. Okamoto, S. Sato, T. Satow, S. Sudo, S. Tanahashi, K Yamazaki, M Fujiwara and O. Motojima,
An Overview of the Large Helical Device Project; Oct 1998
(IAEA-CN-69/OV1/4)

NIFS-572 M. Fujiwara, H. Yamada, A Ejiri, M. Emoto, H. Funaba, M. Goto, K. Ida, H Idei, S. Inagaki, S. Kado, O Kaneko, K Kawahata, A Komori, S. Kubo, R. Kumazawa, S. Masuzaki, T. Minami, J. Miyazawa, T. Morisaki, S. Morita, S Murakami, S. Muto, T Muto, Y. Nagayama, Y Nakamura, H. Nakanishi, K Narihara, K Nishimura, N Noda, T. Kobuchi, S Ohdachi, N. Ohyabu, Y. Oka, M. Osakabe, T. Ozaki, B. J. Peterson, A Sagara, S Sakakibara, R Sakamoto, H. Sasao, M Sasao, K Sato, M. Sato, T. Seki, T Shimozuma, M. Shoji, H. Sazuki, Y Takeiri, K Tanaka, K Toi, T Tokuzawa, K Tsumori, I. Yamada, S Yamaguchi, M. Yokoyama, K.Y Watanabe, T. Watari, R. Akiyama, H. Chikaraishi, K Haba, S Hamaguchi, M. Iima, S. Imagawa, N. Inoue, K Iwamoto, S. Kitagawa, Y. Kubota, J. Kodaira, R. Maekawa, T. Mito, T. Nagasaka, A Nishimura, Y. Takita, C Takahashi, K Takahata, K Yamauchi, H. Tamura, T Tsuzuki, S Yamada, N Yanagi, H Yonezu, Y. Hamada, K Matsuoka, K Murai, K Ohkubo, I. Ohtake, M. Okamoto, S Sato, T. Satow, S Sudo, S Tanahashi, K Yamazaki, O Motojima and A Iiyoshi,
Plasma Confinement Studies in LHD; Oct 1998
(IAEA-CN-69/EX2/3)

NIFS-573 O. Motojima, K Akaishi, H Chikaraishi, H. Funaba, S Hamaguchi, S Imagawa, S Inagaki, N. Inoue, A Iwamoto, S Kitagawa, A Komori, Y. Kubota, R. Maekawa, S Masuzaki, T. Mito, J Miyazawa, T Morisaki, T Muroga, T. Nagasaka, Y. Nakmura, A Nishimura, K Nishimura, N. Noda, N. Ohyabu, S Sagara, S. Sakakibara, R Sakamoto, S Satoh, T Satow, M. Shoji, H Suzuki, K Takahata, H. Tamura, K Watanabe, H Yamada, S. Yamada, S. Yamaguchi, K Yamazaki, N Yanagi, T. Baba, H. Hayashi,

M. Iima, T Inoue, S. Kato, T. Kato, T Kondo, S. Moriuchi, H. Ogawa, I. Ohtake, K Ooba, H. Sekiguchi, N. Suzuki, S. Takami, Y. Taniguchi, T. Tsuzuki, N. Yamamoto, K Yasui, H. Yonezu, M. Fujiwara and A. Iiyoshi,
Progress Summary of LHD Engineering Design and Construction; Oct. 1998
(IAEA-CN-69/FT2/1)

NIFS-574 K Toi, M. Takechi, S. Takagi, G. Matsunaga, M. Isobe, T. Kondo, M. Sasao, D.S. Darrow, K Ohkuni, S. Ohdachi, R. Akiyama A. Fujisawa, M. Gotoh, H. Idei, K Ida, H. Iguchi, S. Kado, M. Kojima, S. Kubo, S. Lee, K Matsuoka, T. Minami, S. Morita, N. Nikai, S. Nishimura, S. Okamura, M. Osakabe, A. Shimizu, Y. Shirai, C. Takahashi, K Tanaka, T. Watari and Y. Yoshimura,
Global MHD Modes Excited by Energetic Ions in Heliotron/Torsatron Plasmas;Oct. 1998
(IAEA-CN-69/EXP1/19)

NIFS-575 Y. Hamada, A. Nishizawa, Y. Kawasumi, A. Fujisawa, M. Kojima, K Narihara, K Ida, A. Ejiri, S. Ohdachi, K Kawahata, K Toi, K Sato, T. Seki, H. Iguchi, K Adachi, S. Hidekuma, S.Hirokura, K Iwasaki, T. Ido, R. Kumazawa, H. Kuramoto, T. Minami, I. Nomura, M. Sasao, K.N. Sato, T. Tsuzuki, I. Yamada and T. Watari,
Potential Turbulence in Tokamak Plasmas;Oct. 1998
(IAEA-CN-69/EXP2/14)

NIFS-576 S. Murakami, U. Gasparino, H. Idei, S. Kubo, H. Maassberg, N. Marushchenko, N. Nakajima, M. Romé and M. Okamoto,
5D Simulation Study of Suprathermal Electron Transport in Non-Axisymmetric Plasmas;Oct. 1998
(IAEA-CN-69/THP1/01)

NIFS-577 S. Fujiwara and T. Sato,
Molecular Dynamics Simulation of Structure Formation of Short Chain Molecules; Nov. 1998

NIFS-578 T Yamagishi,
Eigenfunctions for Vlasov Equation in Multi-species Plasmas Nov. 1998

NIFS-579 M. Tanaka, A. Yu Grosberg and T. Tanaka,
Molecular Dynamics of Strongly-Coupled Multichain Coulomb Polymers in Pure and Salt Aqueous Solutions; Nov. 1998

NIFS-580 J. Chen, N. Nakajima and M. Okamoto,
Global Mode Analysis of Ideal MHD Modes in a Heliotron/Torsatron System: I. Mercier-unstable Equilibria;Dec. 1998

NIFS-581 M. Tanaka, A. Yu Grosberg and T. Tanaka,
Comparison of Multichain Coulomb Polymers in Isolated and Periodic Systems: Molecular Dynamics Study; Jan. 1999

NIFS-582 V.S. Chan and S. Murakami,
Self-Consistent Electric Field Effect on Electron Transport of ECH Plasmas; Feb. 1999

NIFS-583 M. Yokoyama, N. Nakajima, M. Okamoto, Y. Nakamura and M. Wakatani,
Roles of Bumpy Field on Collisionless Particle Confinement in Helical-Axis Heliotrons;Feb. 1999

NIFS-584 T.-H. Watanabe, T Hayashi, T. Sato, M. Yamada and H. Ji,
Modeling of Magnetic Island Formation in Magnetic Reconnection Experiment;Feb. 1999

NIFS-585 R. Kumazawa, T. Mutoh, T. Seki, F. Shinpo, G. Nomura, T. Ido, T. Watari, Jean-Marie Noterdaeme and Yangping Zhao,
Liquid Stub Tuner for Ion Cyclotron Heating, Mar. 1999

NIFS-586 A. Sagara, M. Iima, S. Inagaki, N. Inoue, H. Suzuki, K Tsuzuki, S. Masuzaki, J. Miyazawa, S. Morita, Y. Nakamura, N. Noda, B. Peterson, S. Sakakibara, T. Shimozuma, H. Yamada, K Akaishi, H. Chikaraishi, H. Funaba, O. Kaneko, K Kawahata, A. Komori, N. Ohyabu, O. Motojima, LHD Exp. Group 1, LHD Exp. Group 2,
Wall Conditioning at the Starting Phase of LHD; Mar. 1999

NIFS-587 T. Nakamura and T. Yabe,
Cubic Interpolated Propagation Scheme for Solving the Hyper-Dimensional Vlasov-Poisson Equation in Phase Space;Mar. 1999

NIFS-588 W.X. Wnag, N. Nakajima, S. Murakami and M. Okamoto,
An Accurate δf Method for Neoclassical Transport Calculation ; Mar. 1999

NIFS-589 K Kishida, K Araki, S. Kishiba and K Suzuki,
Local or Nonlocal? Orthonormal Divergence-free Wavelet Analysis of Nonlinear Interactions in Turbulence;Mar. 1999

NIFS-590 K. Araki, K. Suzuki, K. Kishida and S. Kishiba
Multiresolution Approximation of the Vector Fields on T^3 Mar 1999

NIFS-591 K. Yamazaki, H. Yamada K.Y Watanabe, K. Nishimura S. Yamaguchi, H Nakanishi, A. Komori, H. Suzuki, T Mito, H Chikaraishi, K Murai, O Motojima and the LHD Group,
Overview of the Large Helical Device (LHD) Control System and Its First Operation; Apr 1999

NIFS-592 T Takahashi and Y Nakao,
Thermonuclear Reactivity of D-T Fusion Plasma with Spin-Polarized Fuel; Apr 1999

NIFS-593 H Sugama,
Damping of Toroidal Ion Temperature Gradient Modes, Apr 1999

NIFS-594 Xiaodong Li,
Analysis of Crowbar Action of High Voltage DC Power Supply in the LHD ICRF System, Apr 1999

NIFS-595 K. Nishimura, R. Horiuchi and T Sato,
Drift-kink Instability Induced by Beam Ions in Field-reversed Configurations, Apr. 1999

NIFS-596 Y. Suzuki, T-H. Watanabe, T Sato and T Hayashi,
Three-dimensional Simulation Study of Compact Toroid Plasmoid Injection into Magnetized Plasmas; Apr. 1999

NIFS-597 H. Sanuki, K Itoh, M Yokoyama, A Fujisawa, K Ida, S. Toda, S-I Itoh, M Yagi and A Fukuyama,
Possibility of Internal Transport Barrier Formation and Electric Field Bifurcation in LHD Plasma, May 1999

NIFS-598 S. Nakazawa, N. Nakajima, M. Okamoto and N. Ohyabu,
One Dimensional Simulation on Stability of Detached Plasma in a Tokamak Divertor, June 1999

NIFS-599 S. Murakami, N. Nakajima, M. Okamoto and J. Nhrenberg,
Effect of Energetic Ion Loss on ICRF Heating Efficiency and Energy Confinement Time in Heliotrons; June 1999

NIFS-600 R. Horiuchi and T. Sato,
Three-Dimensional Particle Simulation of Plasma Instabilities and Collisionless Reconnection in a Current Sheet;; June 1999

NIFS-601 W. Wang, M. Okamoto, N. Nakajima and S. Murakami,
Collisional Transport in a Plasma with Steep Gradients; June 1999

NIFS-602 T. Mutoh, R. Kumazawa, T. Saki, K. Saito, F Simpo, G. Nomura, T Watari, X. Jikang, G. Cattanei, H Okada, K. Ohkubo, M. Sato, S. Kubo, T. Shimozuma, H. Idei, Y Yoshimura, O. Kaneko, Y Takeiri, M. Osakabe, Y. Oka, K Tsumori, A Komori, H. Yamada, K. Watanabe, S. Sakakibara, M Shoji, R. Sakamoto, S. Inagaki, J Miyazawa, S. Morita, K. Tanaka, B.J Peterson, S. Murakami, T. Minami, S. Ohdachi, S. Kado, K. Narihara, H Sasao, H. Suzuki, K. Kawahata, N. Ohyabu, Y. Nakamura, H. Funaba, S. Masuzaki, S. Muto, K. Sato, T. Morisaki, S. Sudo, Y. Nagayama, T Watanabe. M Sasao, K. Ida, N. Noda, K. Yamazaki, K. Akaishi, A. Sagara, K. Nishimura, T Ozaki, K Toi, O. Motojima, M. Fujiwara, A. Iiyoshi and LHD Exp Group 1 and 2,
First ICRF Heating Experiment in the Large Helical Device; July 1999

NIFS-603 P.C. de Vries, Y. Nagayama, K. Kawahata, S Inagaki, H. Sasao and K. Nagasaki,
Polarization of Electron Cyclotron Emission Spectra in LHD, July 1999

NIFS-604 W Wang, N Nakajima, M. Okamoto and S. Murakami,
δf Simulation of Ion Neoclassical Transport; July 1999

NIFS-605 T. Hayashi, N. Mizuguchi, T Sato and the Complexity Simulation Group,
Numerical Simulation of Internal Reconnection Event in Spherical Tokamak; July 1999

NIFS-606 M Okamoto, N. Nakajima and W Wang,
On the Two Weighting Scheme for δf Collisional Transport Simulation; Aug. 1999

NIFS-607 O. Motojima, A.A. Shishkin, S. Inagaki, K.Y Watanabe,
Possible Control Scenario of Radial Electric Field by Loss-Cone-Particle Injection into Helical Device; Aug. 1999

NIFS-608 R. Tanaka, T. Nakamura and T Yabe,

Constructing Exactly Conservative Scheme in Non-conservative Form; Aug. 1999

NIFS-609 H. Sugama,
Gyrokinetic Field Theory; Aug. 1999

NIFS-610 M. Takechi, G. Matsunaga, S. Takagi, K.Ohkuni, K. Toi, M. Osakabe, M. Isobe, S. Okamura, K. Matsuoka, A. Fujisawa, H. Iguchi, S. Lee, T. Minami, K. Tanaka, Y. Yoshimura and CHS Group;
Core Localized Toroidal Alfven Eigenmodes Destabilized By Energetic Ions in the CHS Heliotron/Torsatron; Sep. 1999

NIFS-611 K. Ichiguchi,
MHD Equilibrium and Stability in Heliotron Plasmas; Sep. 1999

NIFS-612 Y. Sato, M. Yokoyama, M. Wakatani and V. D. Pusovitov.
Complete Suppression of Pfirsch-Schluter Current in a Toroidal l=3 Stellarator; Oct. 1999

NIFS-613 S. Wang, H. Sanuki and H. Sugama,
Reduced Drift Kinetic Equation for Neoclassical Transport of Helical Plasmas in Ultra-low Collisionality Regime; Oct. 1999

NIFS-614 J. Miyazawa, H. Yamada, K. Yasui, S. Kato, N., Fukumoto, M. Nagata and T. Uyama,
Design of Spheromak Injector Using Conical Accelerator for Large Helical Device; Nov. 1999

NIFS-615 M. Uchida, A. Fukuyama, K. Itoh, S.-I. Itoh and M. Yagi,
Analysis of Current Diffusive Ballooning Mode in Tokamaks; Dec. 1999

NIFS-616 M. Tanaka, A.Yu. Grosberg and T. Tanaka,
Condensation and Swelling Behavior of Randomly Charged Multichain Polymers by Molecular Dynamics Simulations; Dec. 1999

NIFS-617 S. Goto and S. Kida,
Sparseness of Nonlinear Coupling; Dec. 1999

NIFS-618 M.M. Skoric, T. Sato, A. Maluckov and M.S. Jovanovic,
Complexity in Laser Plasma Instabilities Dec. 1999

NIFS-619 T.-H. Watanabe, H. Sugama and T. Sato,
Non-dissipative Kinetic Simulation and Analytical Solution of Three-mode Equations of Ion Temperature Gradient Instability; Dec. 1999

NIFS-620 Y. Oka, Y. Takeiri, Yu.I.Belchenko, M. Hamabe, O. Kaneko, K. Tsumori, M. Osakabe, E. Asano, T. Kawamoto, R. Akiyama,
Optimization of Cs Deposition in the 1/3 Scale Hydrogen Negative Ion Source for LHD-NBI System ;Dec. 1999

NIFS-621 Yu.I. Belchenko, Y. Oka, O. Kaneko, Y. Takeiri, A. Krivenko, M. Osakabe, K. Tsumori, E. Asano, T. Kawamoto, R. Akiyama,
Recovery of Cesium in the Hydrogen Negative Ion Sources; Dec. 1999

NIFS-622 Y. Oka, O. Kaneko, K. Tsumori, Y. Takeiri, M. Osakabe, T. Kawamoto, E. Asano, and R. Akiyama,
H- Ion Source Using a Localized Virtual Magnetic Filter in the Plasma Electrode: Type I LV Magnetic Filter: Dec. 1999

NIFS-623 M. Tanaka, S. Kida, S. Yanase and G. Kawahara,
Zero-absolute-vorticity State in a Rotating Turbulent Shear Flow; Jan. 2000

NIFS-624 F. Leuterer, S. Kubo,
Electron Cyclotron Current Drive at $\omega \approx \omega_c$ with X-mode Launched from the Low Field Side; Feb. 2000

NIFS-625 K. Nishimura,
Wakefield of a Charged Particulate Influenced by Emission Process of Secondary Electrons; Mar. 2000